This document is the Accepted Manuscript version of a Published Work that appeared in final form in The Journal of Physical Chemistry C, copyright © American Chemical Society after peer review and technical editing by the publisher. To access the final edited and published work see http://pubs.acs.org/articlesonrequest/AOR-SuCPVqux83DGnf2gFBTb.

Electronic Properties of Biphenylthiolates on Au(111): The Impact of Coverage Revisited

*Elisabeth Verwüster †, Oliver T. Hofmann †, David A. Egger †,§, and Egbert Zojer *†*

† Institute of Solid State Physics, NAWI Graz, Graz University of Technology, Petersgasse 16, 8010 Graz, Austria

§ Department of Materials and Interfaces, Weizmann Institute of Science, Rehovoth 76100, Israel

***Corresponding Author:** Egbert Zojer, egbert.zojer@tugraz.at

Abstract

We study the impact of coverage on the electronic structure of substituted biphenylthiolate-based self-assembled monolayers (SAMs) on Au(111) surfaces with a particular focus on SAM-induced work-function changes, $\Delta\Phi$. This is done using density-functional theory accounting also for van der Waals interactions. We find that the tilt angle of the molecules increases significantly when reducing the coverage, which results in a marked decrease of the perpendicular component of the molecular dipole moment. However, $\Delta\Phi$ does not follow the trend that one would expect on purely geometrical grounds. While for donor-substituted SAMs, $\Delta\Phi$ decreases much more slowly than anticipated, for acceptor-substituted SAMs, the coverage-induced reduction of $\Delta\Phi$ is clearly more pronounced than expected. In fact, in that case $\Delta\Phi$ already vanishes around half coverage. This is in part associated with the (coverage-dependent) bond-dipole originating from the "Au-S-C" bond. Especially for low coverages, however, the relevance of the "Au-S-C" dipole diminishes and we observe a significant contribution of Pauli-pushback (also known as "cushion effect") to the interfacial charge-rearrangements, an effect that hitherto received only minor attention in the discussion of covalently bonded SAMs.

KEYWORDS Self Assembled Monolayers, Coverage, Pauli Push-Back, work function, biphenylthiolate, bond dipole, density-functional theory

Introduction

There is an increasing use of organic self-assembled monolayers (SAMs) covalently bonded to metal surfaces in various organic electronics applications.[1–8] This raises the need for an in-depth understanding of the processes that determine the properties of the resulting metal-organic interfaces.[9–12] Especially molecules with conjugated, rigid backbones are of interest as due to their π-conjugation they allow for moderate tunnel barriers at the metal-organic interface.[13–15] Thus, an interesting class of molecules for tuning charge injection/extraction barriers[8,16,17] in organic devices are oligophenylenethiolates substituted with polar tail-groups to modify the substrate work function, Φ.[18–22] Such systems are at the heart of the present paper (see Figure 1a).

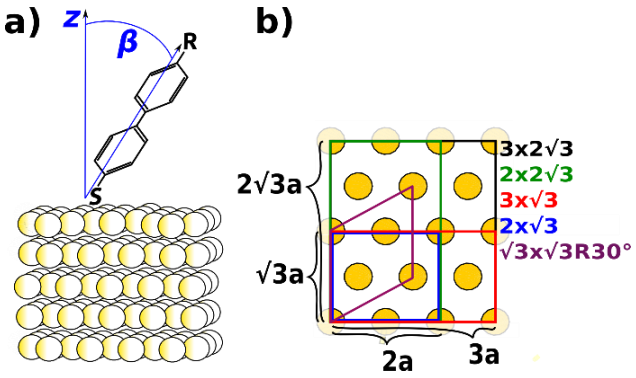

Figure 1: a) schematic sketch of the substituted biphenylthiolate on a slab of five layers of gold. z denotes the axis perpendicular to the slab, β the tilt-angle between long-molecular axis and z, and R = CN, CF_3, CH_3, NH_2 (where data for the CF_3 and CH_3 substituted molecules are shown in the SUI only). b) surface unit cells used in the present study to simulate coverages of 1.0, 0.75, 0.5, 0.375, and 0.25; each unit cell contains one molecule (see text for details).

The impact of the film quality on the monolayer properties is a crucial aspect when comparing idealized perfectly ordered and infinitely extended monolayers with more realistic systems, which are encountered, e.g., on top of the electrodes in actual devices. Quantum-mechanical simulations typically study perfectly ordered and densely-packed metal-SAM systems, because their 2D-periodic nature is compatible with highly-efficient theoretical approaches based on density-functional theory (DFT). For these systems extraordinarily large changes of the work-function, $\Delta\Phi$, and injection barrier amounting up to several eV have been predicted.[23–29] Quantitative agreement between theory and experiment has, however, been achieved only for exceptionally well-ordered layers that induce moderate work-function shifts.[30,31] This calls for developing a systematic understanding of how imperfections in the structural arrangement of the SAM affect the electronic properties of the interface. Indeed, the impact of certain types of film imperfections has been recognized earlier. For instance, Otálvaro et al. studied the influence of deviations from a perfectly flat Au(111) surface.[32] For simple aliphatic thiolates on Au and Ag they, however, found only a minor impact on $\Delta\Phi$. Beyond that, grain-boundaries[33] can have a significant influence on the internal film structure.[34] They are frequently caused by coverage dependent[35] internal stress exerted on the molecular layer by the enforced hexagonal arrangement of the thiolate docking groups. Moreover, incomplete coverage SAMs and "lying-down" (face-on) phases (*vide infra*) have been observed for films grown on small-grained Au substrates.[36] Recently, low-coverage SAMs have even been prepared on purpose to tune/switch the tilt angle of the adsorbed molecules thereby tune $\Delta\Phi$.[37,38]

Most papers modelling the impact of varying densities of molecules bearing polar substituents deal with essentially upright-standing SAMs also when the monolayer-coverage is reduced.[39–43] While this provides significant fundamental insight, it does not necessarily reflect the situation occurring in an actual monolayer at low packing densities. In fact, lying-down phases

of low-coverage SAMs have been found in several experiments,[44–48] which is not surprising considering the significant van der Waals (vdW) attraction between organic adsorbates and metal surfaces.[49,50]

To provide insight into the interplay between coverage, molecular tilt and the electronic properties of the interfaces, we here fully optimize film structures of substituted 4-mercaptobihphenylthiole as a function of coverage using an advanced optimization tool. This allows us to identify the significant impact that the increasing molecular tilt at low coverages has on the SAM-induced work-function modification, $\Delta\Phi$. We show that the "falling over" of molecules causes rather unexpected findings such as a vanishing $\Delta\Phi$ already at half coverage for acceptor substituted layers.

Methodology

Computational approach

The calculations rely on the slab-type band-structure approach, employing density-functional theory using the VASP code.[51] The cut-off energy for the plane-wave basis was set to 273.894 eV and tight convergence criteria of 10^{-6} eV were employed for the SCF procedure. Throughout this work, we used the Perdew-Burke-Ernzerhof (PBE) functional,[52] augmented by the Tkatchenko-Scheffler scheme,[53] in the parameterization that is specifically tailored to surfaces[54] to account for the missing long range van-der-Waals interactions. For that we used the implementation described in [55]. We applied the projector augmented-wave (PAW) method[56,57] to describe valence-core interactions. More details on the PAW potentials used here can be found in the SUI.

At full coverage, we used an 8x8x1 Monkhorst-Pack[58] type-k-point grid that was appropriately scaled for reduced coverages. To decouple periodic replicas of the slab, a ~20 Å vacuum gap and a self-consistently determined dipole layer were introduced.[59] The Au(111) surface was represented by a 5-layer slab, where the positions of the atoms in the bottom three layers were kept fixed in the geometry optimization process. The top two layers and the molecule were allowed to relax without any constraints until the remaining forces where smaller than 10^{-2} eV/Å. We applied an optimization scheme based on internal coordinates and the Direct Inversion in the Iterative Subspace (DIIS) algorithm as implemented in the GADGET tool[60] (which in the used implementation also features automated substrate-detection).[61] This and a suitable initialization of the Hessian are important for obtaining reliable geometries at affordable computational costs, as especially the molecular tilt angle changes significantly in the course of geometry optimizations at low coverages.

System set-up

Ordered oligophenylene-thiolates on Au(111) surfaces at full coverage typically grow in a herringbone pattern with two molecules in a 3x√3 surface unit cell.[47,48,62] A possibility to reduce the coverage preserving this herringbone motive would be to add extra rows of gold between the molecules. Adding a single row yields the 4x√3 unit cell with a striped phase that has been observed experimentally for anthraceneselenolates.[63,64] Systematically reducing the coverage even further pursuing that approach is, however, difficult. Thus, we abandoned the herringbone motive and followed a different strategy with a single molecule per unit cell (noteworthy, the trends obtained in this way are fully consistent with those for the accessible herringbone-based structures at full, 0.75, and 0.60, as shown in the SUI). We defined full coverage by a single molecule in a (√3x√3)R30° surface unit-cell (which gives the same area per molecule as 2 molecules in the 3x√3 cell). Subsequently the unit-cell size was increased,

as indicated in Fig. 1 b. The lowest coverage considered was 0.25, corresponding to a 3x2√3 surface unit-cell.

Interestingly, smooth trends are obtained for all quantities considered below, in spite of the fact that the aspect ratios of the unit cells change quite significantly when following this procedure. This, together with the fact that also for the above-described herringbone structures similar trends are obtained, indicates that for the effects discussed here the exact details of the packing motive are not of primary relevance. This finding is important, since the studied monolayer displays a 2D translational periodicity, which will not necessarily be obtained in experimentally investigated low-coverage samples (the ordered lying-down phases mentioned above notwithstanding). Such periodic boundary conditions are, however, necessary for properly describing the metallic substrate in the simulations; they also allow for a straightforward description of collective electrostatic effects, whose consideration is absolutely crucial when studying SAMs.[14,40]

To understand differences between donor- and acceptor-substituted SAMs, we focus here on two 4-mercaptobiphphenyl derivatives with either a –CN (strong acceptor) or $–NH_2$ (strong donor) tail-group substituent. These were shown to display particularly strong coverage-dependent effects.[14,41] The trends obtained when using the more weakly donating, respectively, accepting substituents $–CH_3$ and $–CF_3$ are equivalent. Thus, for the sake of clarity, the plots of the corresponding data are contained only in the Supporting Information.

Results and discussion

The most important parameter to quantify the change of the SAM geometry upon reducing the coverage is the molecular tilt angle, β, defined as the angle between the surface normal (z) and

the long molecular axis (see Fig. 1a). In Fig 2a, we show its evolution when decreasing the coverage, Θ.

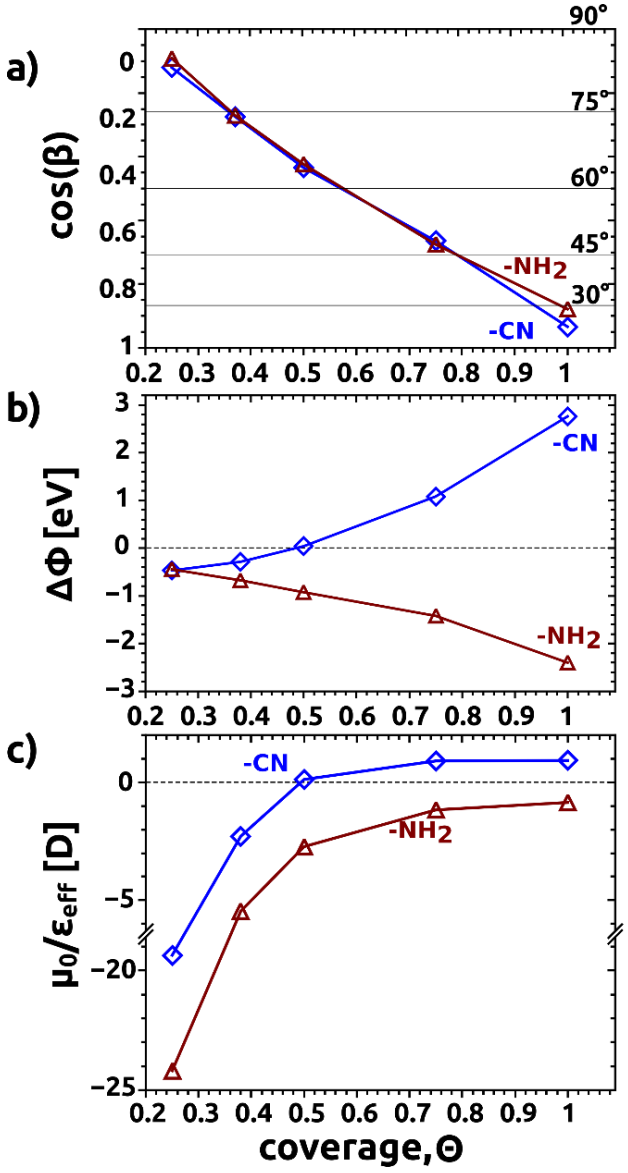

Figure 2: Coverage dependence of a.) the tilt angle (β) and cosine of the tilt angle (cos(β)); b.) the work-function modification, ΔΦ, and c.) the quantity μ_0/ε_{eff} obtained by calculating $\Delta\Phi A_{1.0}\varepsilon_0/(e\Theta\cos(\beta))$, which can be regarded as an effective dipole moment of the combined metal-SAM system (for details see text). Results for the CN-substituted system are shown as blue diamonds; those for the –NH2 substituted case as red triangles.

For both systems, we observe a pronounced increase of β up to point where the molecules "fall over", i.e. they lie essentially flat on the surface and β~90°. To understand how this affects the SAM-induced work-function modification, it is useful remember that ΔΦ is commonly separated into two contributions,[14,17,65–67] denoted here as $\Delta\Phi_{BD}$ and $\Delta\Phi_{mol}$. $\Delta\Phi_{BD}$, arises from the charge rearrangements due to the metal-SAM interactions. As it is commonly associated with bonding, it is referred to as bond dipole. How it is affected by a change in the molecular tilt angle will be discussed later.

Prior to that it is useful to qualitatively analyze how $\Delta\Phi_{mol}$, which stems from the molecular dipole, is affected by a change in β. The molecular dipole and the associated work-function change are related by the Helmholtz equation

$$\Delta\Phi_{mol} = -\frac{e}{\varepsilon_0}\frac{\mu_{z,mol}}{A_{1.0}}\Theta = -\frac{e}{\varepsilon_0}\frac{\mu_{0,mol}\cos(\beta)}{\varepsilon_{eff}A_{1.0}}\Theta \qquad (1)$$

Here ε_0 is the vacuum permittivity and $A_{1.0}$ is the surface area per molecule at Θ=1.0. In the present case with one molecule per unit cell, $A_{1.0}$ is also the area of the (√3x√3)R30° surface unit-cell, which amounts to 22.27Å^2. The area per molecule at reduced coverages is then given by A_1/Θ. $\mu_{z,mol}$ is the (coverage dependent) z-component of the dipole moment per molecule within the monolayer. The sign of $\mu_{z,mol}$ is taken to be positive, when the dipole moment points away from the substrate. $\mu_{z,mol}$ includes depolarization effects that originate from the polarization of the molecular electron cloud caused by the electrical fields of the surrounding molecules.[41–43,68–70] Note that these depolarization effects are intrinsically considered in our self-consistent calculations.

In the right part of Eq. (1), the expression is recast in terms of the intrinsic (gas-phase) dipole moment of the isolated molecule, $\mu_{0,mol}$. The appearance of cos(β) in the right part of Eq. (1)

denotes that only the z- (i.e. perpendicular) component of the molecular dipole moment impacts the value of $\Delta\Phi$. In passing we note that for the actual SAM on a metal-substrate the in-plane (x- and y-) components of the dipoles of the unit cell have to disappear, as a metal does not tolerate a potential gradient parallel to its surface, i.e., the corresponding dipole components of the molecule will be compensated by a polarization of the metal substrate (described by mirror charges). On more technical grounds, when applying periodic boundary conditions, the in-plane components of the molecular dipole moment in the SAM disappear also in the isolated monolayer as a consequence of the translational symmetry.

ε_{eff} is a coverage-dependent effective parameter that quantifies the decrease in the dipole moment due to depolarization effects.[41] At full coverage it is often approximated by the dielectric constant of a bulk material consisting of the same molecules as the SAM. At lower coverages ε_{eff} decreases, accounting for the fact that depolarization diminishes.[41] Finally it should be noted that in the following discussions we will frequently refer to $|\Delta\Phi_{mol}|$, where the absolute value is used because the sign of $\Delta\Phi_{mol}$ (respectively, the orientation of the dipole on the surface) differs for donor and acceptor substituents.

When decreasing Θ, $|\Delta\Phi_{mol}|$ is expected to decrease as well for two reasons: (i) the dipole density naturally decreases with decreasing molecular density, and (ii) at low coverage the tilt angle increases (see Fig. 2a). This results in a smaller component of the dipole moment perpendicular to the surface as expressed through $\cos(\beta)$ in Eq. (1). The trend is counteracted by a decreasing depolarization at reduced coverage, but this effect is smaller than the two aforementioned ones (vide infra).

For both Au-SAM systems, the DFT-calculated evolution of (the total) work-function change, $\Delta\Phi$, as a function of Θ is shown in Fig. 2b. For the -NH_2 substituted SAM, $|\Delta\Phi|$ decreases with

coverage as qualitatively expected from the above considerations regarding the molecular contribution, $|\Delta\Phi_{mol}|$. What can, however not be explained in terms of molecular electrostatics alone is that a significant value of $|\Delta\Phi|$ (0.44 eV) still remains at 0.25 coverage, when the molecules lie almost flat on the surface (cf. Fig. 2a)). For the –CN case, the dependence of $|\Delta\Phi|$ on Θ deviates even more significantly from the trend arising from the molecular dipole: A decrease of $|\Delta\Phi|$ is observed only for $\Theta>0.5$; at $\Theta=0.5$, $|\Delta\Phi|$ vanishes and $\Delta\Phi$ even changes sign for lower coverages reaching essentially the same value as in the –NH2 substituted SAM at $\Theta=0.25$.

The deviation of the behavior of the actual interface from that of an assembly of conventional dipoles can be illustrated more clearly by calculating

$$\frac{\mu_0}{\varepsilon_{eff}} = \frac{\Delta\Phi\, A_{1.0}\, \varepsilon_0}{e\,\Theta\cos(\beta)} \qquad (2)$$

It can be regarded as the quantity one obtains when modelling the metal-SAM system by an effective dipole moment pointing in the same direction as the long molecular axis. If the molecular dipoles were the only reason for $\Delta\Phi$ and in the absence of depolarization effects the coverage dependence of μ_0/ε_{eff} should yield a horizontal line. For systems in which depolarization is significant, which typically applies to SAMs,[28] $|\Delta\Phi|$ should increase at small coverages. Qualitatively, this expectation is met for the $–NH_2$ substituted SAM, but even in that system depolarization-related effects can hardly account for the increase of μ_0/ε_{eff} by a factor of ~28 between $\Theta=1.0$ and $\Theta=0.25$ (note the axis break in Fig. 2c)). In the –CN substituted SAMs a behavior differing even qualitatively from the expectations for conventional dipoles with a sign-change at $\Theta=0.5$ is found (see Fig. 2c)).

These considerations show that the behavior of the actual system significantly deviates from that of an assembly of conventional dipoles aligned along the long molecular axes. This means that the second contribution to $\Delta\Phi$, which is the above-mentioned interfacial charge-rearrangement related work-function shift, $\Delta\Phi_{BD}$, must display a peculiar coverage dependence. In this context, it is interesting to mention that, when previously studying the coverage-dependence for an analogous –CN substituted SAM on Au(111) at small (essentially constant) molecular tilt angles, a vanishing or even negative value of $\Delta\Phi$ was not observed.[41] This implies that the peculiar evolution of $\Delta\Phi_{BD}$ must be rooted in the "falling-over" of the molecules at low coverages.

For thiolate-bonded SAMs, $\Delta\Phi_{BD}$ is frequently associated with the charge rearrangements due to the formation of a chemical bond between the thiols and the metal-surface, which can be viewed as the replacement of the S-H bonds by S-Au bonds[71] or as the formation of a bond between the –S* radical and the Au surface[65] (for a comparison of the two views see [72]). We, here, refrain from a numerical evaluation of the coverage dependence of $\Delta\Phi_{BD}$, as, when adopting the "bond-replacement" point of view in systems with changing tilt angles, the relevant information is masked by the dependence of the S-H dipole on the on the tilt and on the relative position of the H atom.[72] For the "bond-formation approach" one mostly analyzes the charge-rearrangements that originate from the transition from an open to a closed-shell electronic structure of the adsorbed molecules. I.e., in this case the sought-after bonding-related charge-redistributions at the metal-molecule interface are superimposed with those associated with the loss of radical character of the adsorbing molecules.[72]

Instead, we adopt a different approach to more clearly elucidate the reason for the peculiar coverage dependence of $\Delta\Phi_{BD}$: In a *gedankenexperiment* we simply eliminate the contribution of the charge rearrangements associated with the thiolate by replacing it with a hydrogen atom.

This is indicated in the inset of Fig. 3a. To achieve this technically, only the geometric parameters of the C-H bond replacing the C-S bond are optimized. We denote quantities calculated for the surrogate system with primes (‘). The, differences in the evolution of the work-function change due to this hypothetical model system and the complete SAM can be associated with the contribution of the Au-thiolate bond to $\Delta\Phi_{BD}$. As the smallest Au-H distance is 2.24 Å, the “chemical” contributions of the interaction between the extra H-atom and the surface to $\Delta\Phi_{BD}$’ can be expected to be very small. Interestingly, as shown in Fig. 3a, when calculating the coverage dependence of $\Delta\Phi$’, one obtains an evolution qualitatively very similar to that of $\Delta\Phi$ shown in Fig. 2b. Only at full coverage, where the density of thiolate-Au bonds is highest, $\Delta\Phi$ is clearly less positive (more negative) than $\Delta\Phi$’ for the –CN (-NH_2) substituted SAM (cf., Fig. 2b and Fig. 3a). This comparison shows that the main reason for the deviation between the “conventional” polarizable dipole picture sketched in Eq. (1) and the actual evolution of $\Delta\Phi$ when approaching the dilute limit is not directly related to the Au-S bond formation.

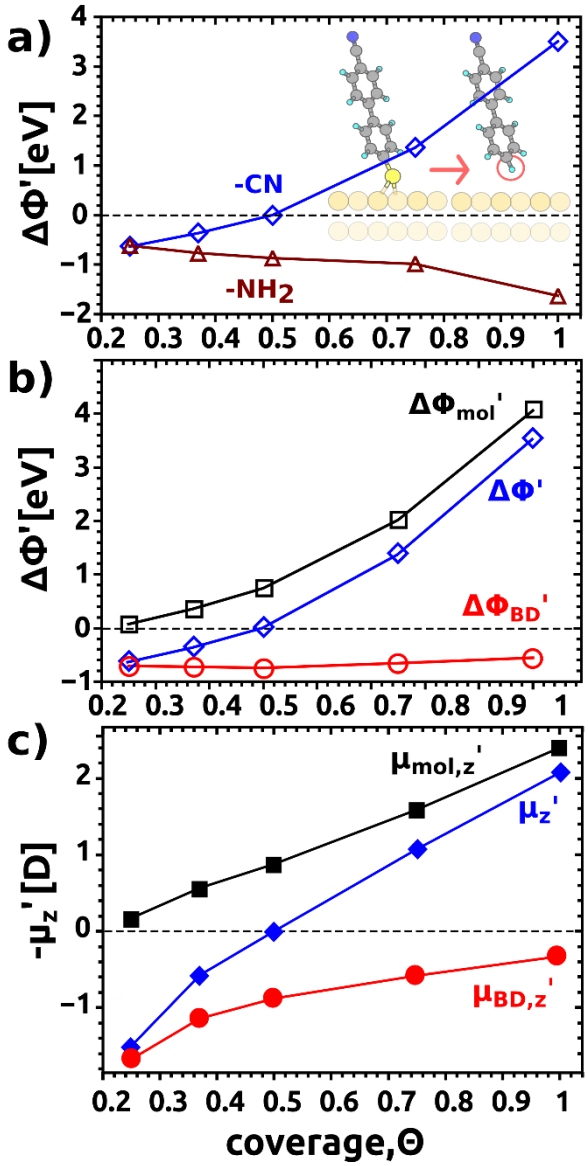

Figure 3: a) Coverage-dependence of the work function-modification in the hydrogen-substituted model systems bearing -CN (blue diamonds) and -NH_2 (red triangles) tail groups. The inset shows the substitution of the sulfur by a hydrogen atom as part of our gedankenexperiment; b) coverage-dependent decomposition of the total work-function change in the –CN substituted model system, $\Delta\Phi$', (blue diamonds) into contributions from the (free-standing) monolayer, $\Delta\Phi_{mol}$', (black squares) and from the interfacial charge-rearrangements, $\Delta\Phi_{BD}$', (red circles); c) analogous decomposition into contributing dipoles per molecule. The

energetic shifts in b) are proportional to those in c) divided by the surface area per molecule ($\Delta\Phi' \propto \mu_z'\Theta/A_{1.0}$).

An advantage of the chosen model system is that here the individual contributions of $\Delta\Phi_{mol}'$ and $\Delta\Phi_{BD}'$ to $\Delta\Phi'$ can be separated unambiguously.[73] The results for the –CN substituted SAM are shown in Fig. 3b; those for the -NH_2 case are contained in the SUI. As expected (cf., Eq (1)) for polarizable dipoles, $\Delta\Phi_{mol}'$ decreases continuously with decreasing coverage approaching zero for the close to flat-lying molecules at Θ=0.25. Interestingly, the work-function modifications caused by the molecule-metal interaction, $\Delta\Phi_{BD}'$, show essentially no coverage dependence. What this means becomes more evident when considering the corresponding quantities per surface area occupied by each molecule (i.e., per $A_{1.0}/\Theta$). To ensure that the resulting quantities (displayed in Fig. 3c)) represent dipole moments, they are defined as (cf., Eq. (1)):

$$\mu_{X,z}' = \frac{\varepsilon_0}{e}\Delta\Phi_X' \frac{A_{1.0}}{\Theta} \qquad (3)$$

μ_z' (derived from $\Delta\Phi'$) then represents the total dipole moment associated with each molecule, and $\mu_{mol,z}'$, respectively, $\mu_{BD,z}'$ denote the contributions from the molecular dipole and the molecule-substrate interaction. While $|\mu_{mol,z}'|$ decreases strongly with coverage, one sees a pronounced *increase* of $|\mu_{BD,z}'|$ at low coverage (by a factor of ~5 between Θ=1.0 and Θ=0.25). These opposite trends explain, why, for the –CN substituted SAM μ_z' and also $\Delta\Phi'$ disappear at half coverage, where $\mu_{mol,z}'$ and $\mu_{BD,z}'$ cancel, as schematically indicated in the left panel of Fig. 4a. For smaller Θ, the combination of the different orientation of the dipoles and the larger absolute magnitude of $\mu_{BD,z}'$ explain why then the adsorption of the SAM reduces the work

function in spite of the acceptor substituent. In the NH_2-substituted case the absolute value of $\mu_{mol,z}$' and $\mu_{BD,z}$' display a similar coverage dependence as the one discussed above (see SUI). For this case, however, the dipoles add up, and no cancellation of dipole moments or changes in the sign of $\Delta\Phi$' occur. This is illustrated in Fig. 4b. Bearing in mind the similar evolutions of $\Delta\Phi$ and $\Delta\Phi$' (vide supra) with coverage, the strong increase of $\mu_{BD,z}$' at small coverage can also be held responsible for the trends observed for the thiolate-bonded SAMs in Fig. 2 especially at small Θ.

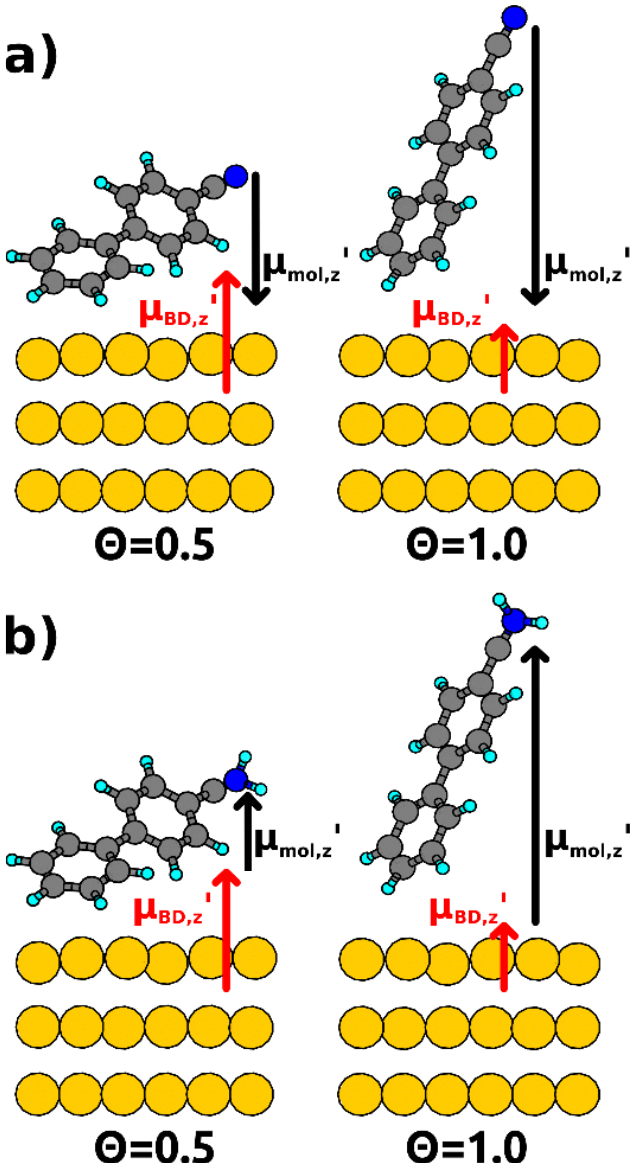

Figure 4: Schematic illustration of the resulting interplay of $\mu_{mol,z}$' and $\mu_{BD,z}$' when going from

full to half coverage for the hydrogen substituted model system either bearing an electron accepting substituent (-CN) (panel a)) or b): an electron donating substituent (-NH_2) (panel b)).

What remains to be explained is the strong increase of $\mu_{BD,z}$' in diluted SAMs. By definition, the bond dipole originates from the charge-rearrangements $\Delta\rho'$ induced by the metal-molecule interaction. For the model system, we define them as

$$\Delta\rho' = \rho'_{sys} - \left(\rho'_{slab} + \rho'_{mol}\right) \qquad (4),$$

with ρ'_{sys} being the electron density of the combined system, ρ'_{slab} the electron density of the metal slab and ρ'_{mol} the electron density of the isolated molecular monolayer. To calculate $\Delta\rho$ for the thiolate-containing systems in the bond-replacement picture (vide supra), one additionally needs to consider the charge-densities associated with the H atoms that are removed in the course of the bond-formation:

$$\Delta\rho = \rho^{sys} - \left(\rho^{slab} + \rho^{mol} + \rho^{H}\right) \qquad (5),$$

For Θ=0.25, the $\Delta\rho$'s for a hydrogen substituted model system and the corresponding thiolate system are compared in Fig 5 (plots for Θ=1.0 and Θ=0.5 are contained in the SUI). Panel 5a provides a side view of both systems, where the plotted quantity corresponds to $\Delta\rho$ integrated over the unit cell in the direction along the viewing axis. In the model as well as in the thiolate system one sees strong charge depletion (blue region) around the molecular backbone accompanied by an accumulation of charge directly underneath the molecule (red region). The charge depletion close to the S-atom is stronger in the actual SAM than that in the C-H region of the model system, an observation to which we will return later.

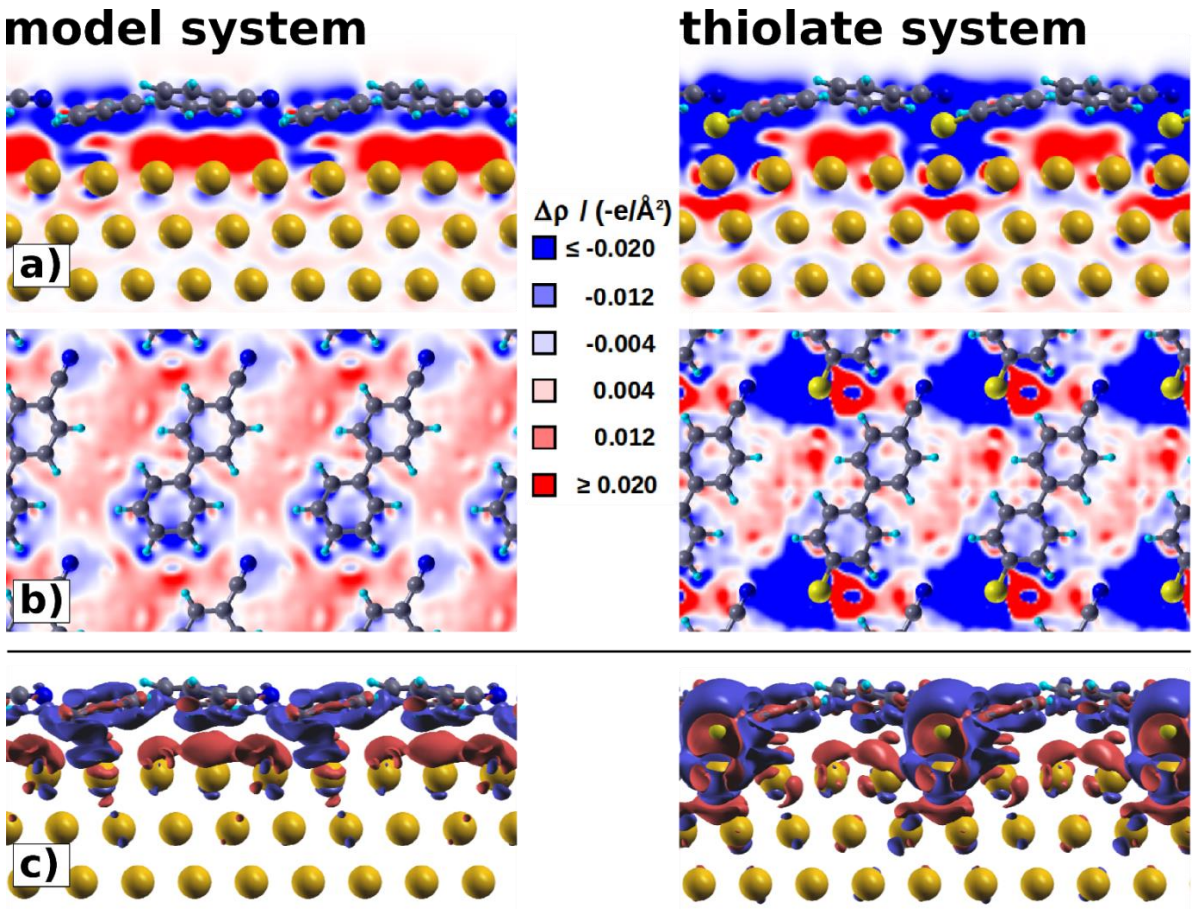

Figure 5: Charge rearrangements arising from the interaction between the metal and the monolayer for the –CN substituted SAMs at Θ=0.25. In the first and central panels a) and b) charge-density redistributions integrated over the unit cell in the viewing direction are shown. Red areas denote charge accumulation, blue areas depletion; only part of the five Au layers of the metal slab are shown. Panel a) contains side views for the H-terminated model system and the corresponding thiolate system. In panel b) the respective top views are shown. Panel c) contains 3D isodensity-plots (with an isovalue of 0.003 e/Å^3).

In Figure 5b, we provide the corresponding top view for both systems, again integrated along the viewing axis. A decrease of (integrated) charge around the molecular backbone can be seen for the thiolate system as well as for the model system (light blue area). An increase of the integrated electron density is seen mostly in the areas between the organic moieties.

Qualitatively, both systems again show the same behavior with the exception of a particular strong charge-depletion (enhancement) close the S-atom of the thiolate.

We attribute the depletion of electron density around the molecular backbone and the concomitant shift to below and between the organic molecules to the so-called Pauli-Pushback effect[9,10,12,74–77] (also termed cushion-effect). It is an effect originating from the repulsion of the overlapping electron densities of the adsorbate layer and the substrate caused by exchange interaction,[77] which leads to a reduction of the surface dipole of the metal substrate. Thus, it results in a significant work-function reduction upon monolayer adsorption. Computationally, it is discernible from direct charge donation from occupied states in the molecules to the metal by an absence of molecular density of states at the Fermi-level.[78] This is indeed the case here (see SUI). While Pauli-pushback is well known in the context of flat lying molecules on various metal surfaces,[10,74–76] it has rarely been considered for covalently bonded SAMs.[44] Still, Nouchi et al. found it to be crucial for understanding the experimental properties of their (intentionally) disordered systems.[37]

Since the extend of Pauli-Pushback (and the concomitant work-function reduction) depends on the magnitude of the overlap of the molecular and substrate's electron clouds, it becomes larger when the distance between the backbone and the surface is reduced. This is the case at low coverage, where the molecular tilt angles increases enormously ("falling over" of the molecules).

We can now return to the main difference between the model system and the thiolate in Fig. 5, which are the strong charge-rearrangements occurring in the vicinity of the S-atoms. As Figure 2b and 3b show, $\Delta\Phi$ is essentially the same at Θ=0.25 for both systems. This indicates that charge rearrangements directly associated with the thiolate-gold bond must have an only minor contribution to $\Delta\Phi$ at low coverage. To understand and corroborate this finding, Fig 5c shows

$\Delta\rho$ without integration in the form of isodensity plots. The charge rearrangements in the vicinity of the thiolate are massive, but to a significant extent are associated with charge redistributions occurring parallel to the surface.[79] Considering that only the components of charge rearrangements perpendicular to the surface contribute to work-function changes one can understand that the S-Au bond formation dominates the interface energetics only at high coverage where the lateral density of thiolates on the surface is large.

SUMMARY AND CONCLUSION

In the present paper, the non-trivial dependence of SAM-induced modification of Au work-functions, $\Delta\Phi$, on molecular coverages has been discussed. While the assembly of –CN substituted 4-mercapto-biphenyls increase the work-function of a Au(111) surface by ~2.8 eV at full coverage, no work-function change is observed for half coverage (Θ=0.5). At lower values of Θ, $\Delta\Phi$ even becomes negative in spite of the strongly electron-accepting character of the –CN group. Conversely, for a donor (i.e., $-NH_2$) substituted SAM $\Delta\Phi$ does not change its sign as a function of coverage and at Θ=0.25 approaches -0.5 eV, which is the same value as for the –CN substituted layer. These observations are shown to be direct consequence of the increased molecular tilt angles occurring at lower coverages, where besides the tilt-angle dependence of the perpendicular component of the molecular dipoles, Pauli-pushback (also termed cushion-effect) plays a crucial role. At low coverages, where the overlap between the π-system of the molecule and the electron-cloud tailing from the metal-surface is largest, it is even the dominant effect determining the SAM-induced work-function change. Based on these insights, we surmise that in imperfectly packed systems of thiolates on a metal surface, the

"SAM-character" (i.e., molecular dipoles and dipoles related to the Au-S bond formation dominating the interface energetics) is increasingly lost and the film properties start resembling those of a rather inert physisorbed molecular monolayer.

ASSOCIATED CONTENT

Supporting Information.

Further details of the computational methodology, additional data for systems with two molecules in the unit cell and for $–CF_3$ and $–CH_3$ substituted SAMs, the partitioning into monolayer and interaction-derived contributions to the work-function change for the $–NH_2$ substituted model system, selected densities of states, and charge rearrangement plots for half and full coverage.

AUTHOR INFORMATION

Corresponding Authors

*Email: egbert.zojer@tugraz.at

Notes

The authors declare no competing financial interests.

ACKNOWLEDGMENT

Financial support by the Austrian Science Fund (FWF): P24666-N20 is gratefully acknowledged. The work of D.A.E. has been partly supported by a DOC fellowship of the Austrian Academy of Sciences. The computational studies presented have been performed

using the clusters of the division for high performance computing at the Graz University of Technology. O.T.H. acknowledges support though the Austrian Science Fund (FWF): J-3285.

ABBREVIATIONS

SAM, self-assembled monolayer; DFT, density-functional theory; vdW, van der Waals

Supporting Information to

Electronic Properties of Biphenylthiolates on Au(111): The Impact of Coverage Revisited.

*Elisabeth Verwüster †, Oliver T. Hofmann †, David A. Egger †,§, and Egbert Zojer *†*

† Institute of Solid State Physics, Graz University of Technology, Petersgasse 16, 8010 Graz, Austria

§ Department of Materials and Interfaces, Weizmann Institute of Science, Rehovoth 76100, Israel

***Corresponding Author:** Egbert Zojer, egbert.zojer@tugraz.at

1. Additional details on the applied methodology.

The Monkhorst-Pack [Monkhorst, H. J.; Pack, J. D. Special Points for Brillouin-Zone Integrations. *Phys. Rev. B* **1976**, *13*, 5188–5192] *k-point* scheme was used in all calculations. Due to the different calculated unit-cells *k*-point meshes were manually chosen for each coverage and checked for convergence, resulting in: 8x8x1, 8x6x1, 8x5x1, 4x6x1 and 4x5x1 for Θ=1, 0.75, 0.50, 0.37 and 0.25.

Table S1: In the present study following PAW potentials were used

Au	PAW_PBE Au 06Sep2000
S	PAW_PBE S 17Jan2003
C	PAW_PBE C_s 06Sep2000
H	PAW_PBE H 15Jun2001
N	PAW_PBE N_s 07Sep2000
F	PAW_PBE F 08Apr2002

To avoid spurious surface reconstructions, the Au(111) lattice constant was set to the equilibrium value for the used methodology, which amounts to 2.928 Å was used.

2. Properties of all investigated thiolate-bonded SAMs

In Figure S1 the dependence of the tit angle, the work-function modification and the effective long-axis dipole are shown for all studied molecules as a function of coverage. It is analogous to Fig. 2 from the main manuscript, but contains data for many more systems.

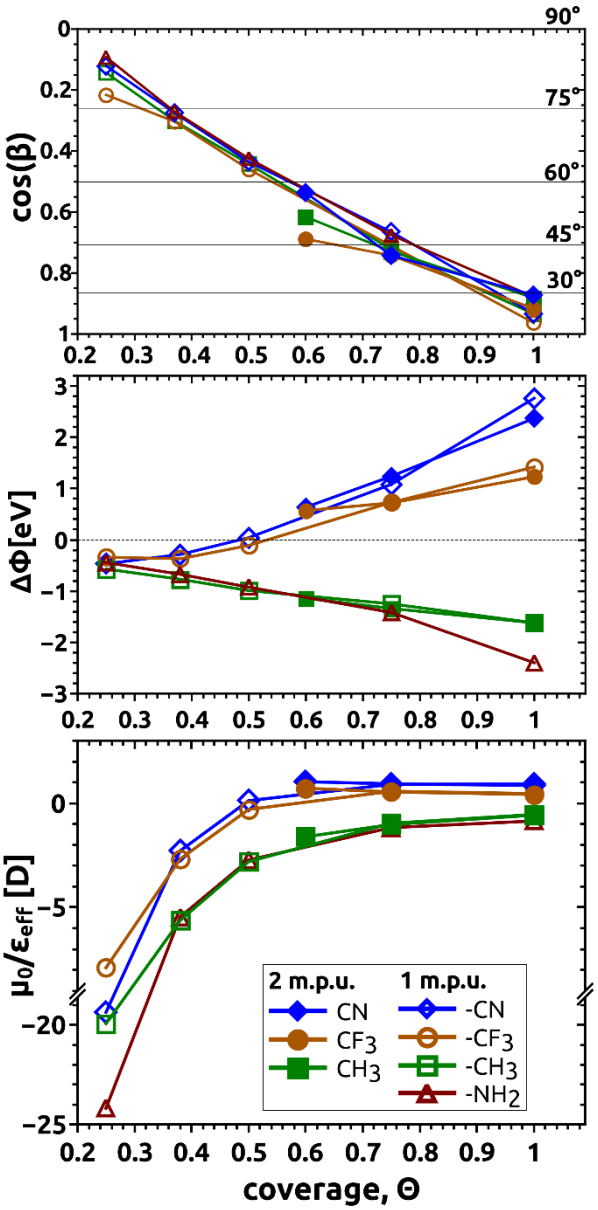

Figure S1: Coverage dependence of a.) the tilt angle (β) and cosine of the tilt angle (cos(β)); b.) the work-function modification, ΔΦ, and c.) the quantity μ_0/ε_{eff} obtained by calculating $\Delta\Phi A_{1.0}\varepsilon_0/(e\Theta\cos(\beta))$, which can be regarded as an effective dipole moment of the combined metal-SAM system. Results for the CN-substituted system are shown as blue diamonds; for $-CF_3$ in brown circles, for CH_3 in green squares and those for the $-NH_2$ substituted case as red triangles. The full symbols denote the unit cells containing two molecules in a herringbone

arrangement.

3. Decomposition of the electronic properties of the H-terminate, NH2 tail-group substitute SAM into monolayer and interaction-based contributions

The following plot corresponds to Fig. 3b) and c) of the main manuscript for the NH_2 instead of CN substituted monolayer.

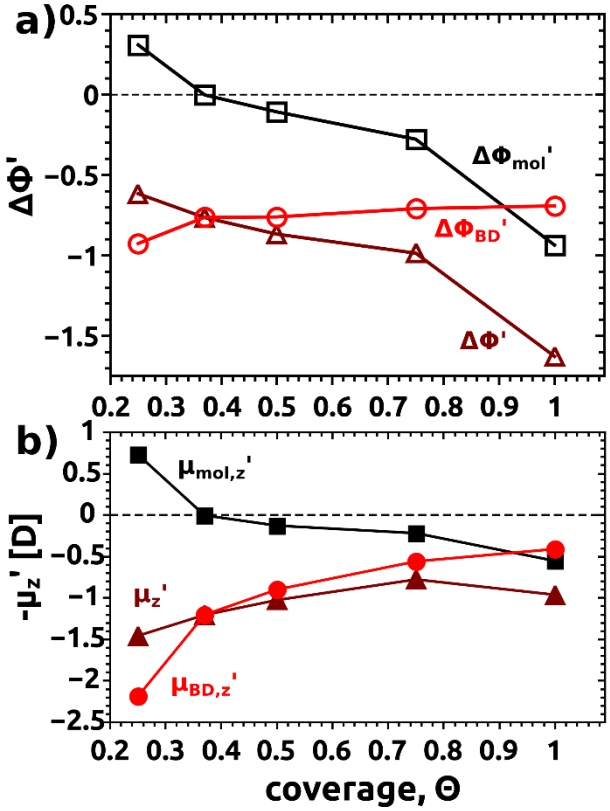

Figure S2: a) coverage-dependent decomposition of the total work-function change in the –NH_2 substituted model system, $\Delta\Phi$', (dark red triangles) into contributions from the (free-standing) monolayer, $\Delta\Phi_{mol}$', (black squares) and from the interfacial charge-rearrangements, $\Delta\Phi_{BD}$', (red circles); b) analogous decomposition into contributing dipoles per molecule. The energetic shifts in a) are proportional to those in b) divided by the surface area per molecule ($\Delta\Phi' \propto \mu_z'\Theta/A_{1.0}$).

There are two differences in the evolution of the monolayer-related quantities $\mu_{mol,z}$' and $\Delta\Phi_{mol,z}$' compared to the case of the –CN substituted SAM in the main manuscript: (i) The different signs at high coverages owing to the donating instead of accepting character of the tail-group substituent. (ii) A change in sign of $\mu_{mol,z}$' and $\Delta\Phi_{mol,z}$' at Θ=0.25, which does not occur in the –CN substituted SAMs. It is the consequence of an off-axis component of the

dipole moment of the substituent caused by the pyramidalization of the bonds in the C-N-H_2 part of the molecule. This component determines the z-component of the monolayer dipole of the essentially flat-lying molecules for the conformation studied here (see Fig. S3). As far as the relative large magnitude of the dipole compared to the dipole of the essentially upright-standing SAM at full coverage is concerned, one needs to keep in mind that at low packing densities depolarization effects are significantly reduced.

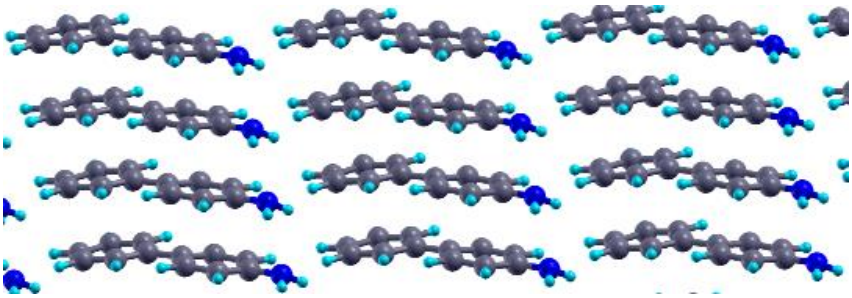

Figure S3: Structure of the isolated H-terminated monolayer of the -NH_2 tail-group substituted monolayer at Θ=0.25 used to calculate $\mu_{mol,z}$' and $\Delta\Phi_{mol,z}$' shown in Fig. S2.

4. Densities of States

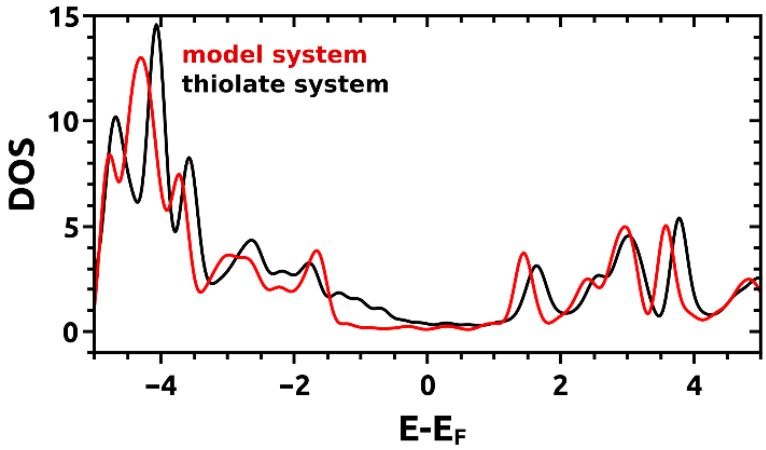

Figure S4: Density of states (DOS) of the –CN substituted model(red) and thiolate(black) systems at Θ=0.25. The energy is plotted relative to the Fermi-energy.

5. Charge-density rearrangements at half and full coverage

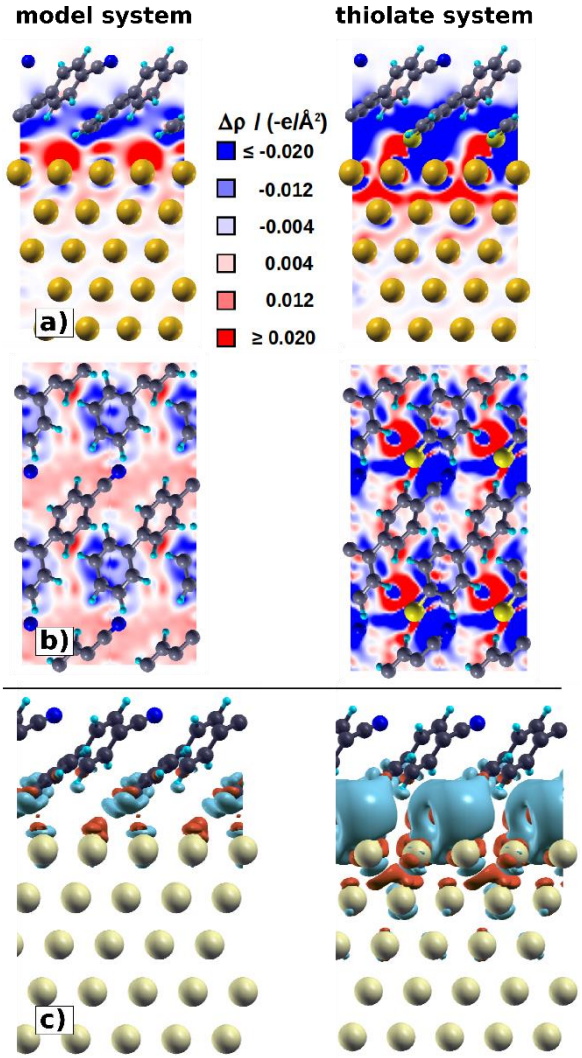

Figure S5: Charge rearrangements arising from the interaction between the metal and the monolayer for the –CN substituted SAMs at Θ=0.5. In the first and central panels a) and b) charge-density redistributions integrated over the unit cell in the viewing direction are shown. Red areas denote charge accumulation, blue areas depletion; only part of the five Au layers of the metal slab are shown. a) contains plots for the H-terminated model system and the corresponding thiolate system in a side-view manner. In panel b) the top view of the integrated charge rearrangements for both the model- and the thiolate-system are shown. Panel c) contains 3D isodensity-plots (with an isovalue of 0.005 e/Å^3).

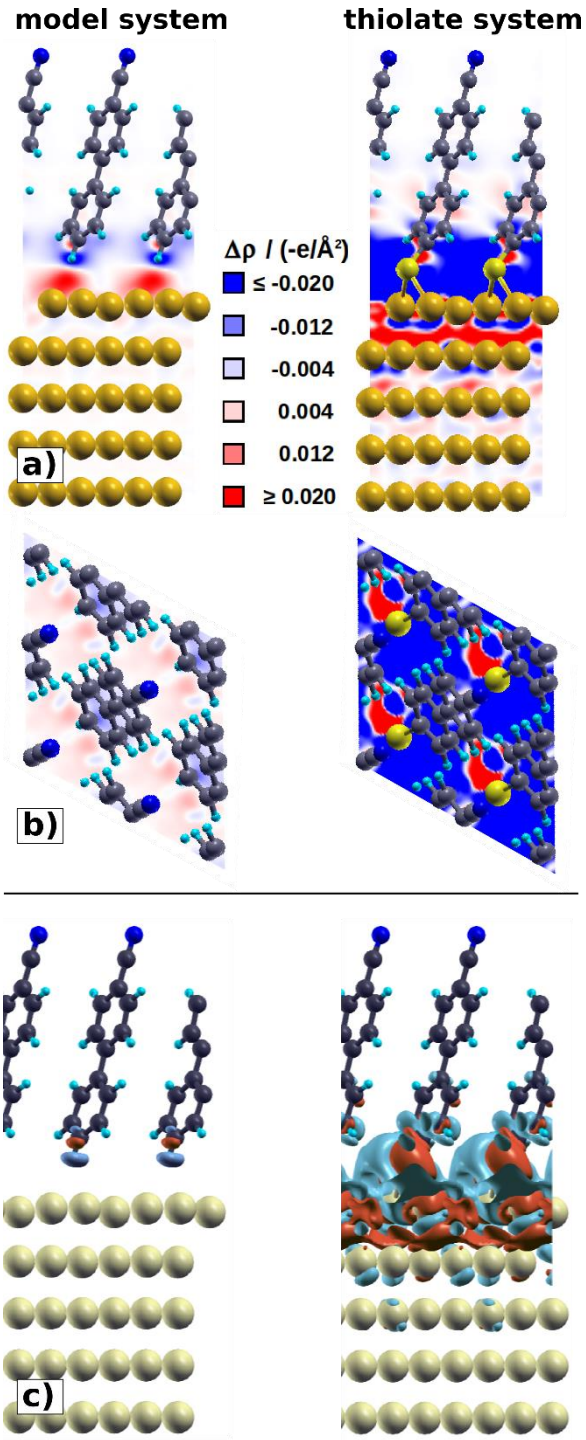

Figure S6: Charge rearrangements arising from the interaction between the metal and the monolayer for the –CN substituted SAMs at Θ=1.0. In the first and central panels a) and b) charge-density redistributions integrated over the unit cell in the viewing direction are shown. Red areas denote charge accumulation, blue areas depletion; only part of the five Au layers of the metal slab are shown. a) contains plots for the H-terminated model system and the

corresponding thiolate system in a side-view manner. In panel b) the top view of the integrated charge rearrangements for both the model- and the thiolate-system are shown. Panel c) contains 3D isodensity-plots (with an isovalue of 0.005 e/Å^3).

References

(1) Margapoti, E.; Li, J.; Ceylan, Ö.; Seifert, M.; Nisic, F.; Anh, T. L.; Meggendorfer, F.; Dragonetti, C.; Palma, C.-A.; Barth, J. V.; et al. A 2D Semiconductor–Self-Assembled Monolayer Photoswitchable Diode. *Adv. Mater.* **2015**.

(2) Kim, C.-H.; Hlaing, H.; Hong, J.-A.; Kim, J.-H.; Park, Y.; Payne, M. M.; Anthony, J. E.; Bonnassieux, Y.; Horowitz, G.; Kymissis, I. Decoupling the Effects of Self-Assembled Monolayers on Gold, Silver, and Copper Organic Transistor Contacts. *Adv. Mater. Interfaces* **2014**.

(3) Crivillers, N.; Osella, S.; Van Dyck, C.; Lazzerini, G. M.; Cornil, D.; Liscio, A.; Di Stasio, F.; Mian, S.; Fenwick, O.; Reinders, F.; et al. Large Work Function Shift of Gold Induced by a Novel Perfluorinated Azobenzene-Based Self-Assembled Monolayer. *Adv. Mater.* **2013**, *25*, 432–436.

(4) Newton, L.; Slater, T.; Clark, N.; Vijayaraghavan, A. Self Assembled Monolayers (SAMs) on Metallic Surfaces (gold and Graphene) for Electronic Applications. *J. Mater. Chem. C* **2013**, *1*, 376.

(5) Halik, M.; Hirsch, A. The Potential of Molecular Self-Assembled Monolayers in Organic Electronic Devices. *Adv. Mater.* **2011**, *23*, 2689–2695.

(6) Ma, H.; Yip, H.-L.; Huang, F.; Jen, A. K.-Y. Interface Engineering for Organic Electronics. *Adv. Funct. Mater.* **2010**, *20*, 1371–1388.

(7) Marmont, P.; Battaglini, N.; Lang, P.; Horowitz, G.; Hwang, J.; Kahn, A.; Amato, C.; Calas, P. Improving Charge Injection in Organic Thin-Film Transistors with Thiol-Based Self-Assembled Monolayers. *Org. Electron.* **2008**, *9*, 419–424.

(8) De Boer, B.; Hadipour, A.; Mandoc, M. M.; van Woudenbergh, T.; Blom, P. W. M. Tuning of Metal Work Functions with Self-Assembled Monolayers. *Adv. Mater.* **2005**, *17*, 621–625.

(9) Braun, S.; Salaneck, W. R.; Fahlman, M. Energy-Level Alignment at Organic/Metal and Organic/Organic Interfaces. *Adv. Mater.* **2009**, *21*, 1450–1472.

(10) Koch, N. Organic Electronic Devices and Their Functional Interfaces. *ChemPhysChem* **2007**, *8*, 1438–1455.

(11) Love, J. C.; Estroff, L. A.; Kriebel, J. K.; Nuzzo, R. G.; Whitesides, G. M. Self-Assembled Monolayers of Thiolates on Metals as a Form of Nanotechnology. *Chem. Rev.* **2005**, *105*, 1103–1170.

(12) Ishii, H.; Sugiyama, K.; Ito, E.; Seki, K. Energy Level Alignment and Interfacial Electronic Structures at Organic/Metal and Organic/Organic Interfaces. *Adv. Mater.* **1999**, *11*, 605–625.

(13) Karthäuser, S. Control of Molecule-Based Transport for Future Molecular Devices. *J. Phys. Condens. Matter* **2011**, *23*, 013001.

(14) Heimel, G.; Rissner, F.; Zojer, E. Modeling the Electronic Properties of Π-Conjugated Self-Assembled Monolayers. *Adv. Mater.* **2010**, *22*, 2494–2513.

(15) Shamai, T.; Ophir, A.; Selzer, Y. Fabrication and Characterization of "on-Edge" Molecular Junctions for Molecular Electronics. *Appl. Phys. Lett.* **2007**, *91*, 102108.

(16) Bock, C.; Pham, D. V.; Kunze, U.; Käfer, D.; Witte, G.; Wöll, C. Improved Morphology and Charge Carrier Injection in Pentacene Field-Effect Transistors with Thiol-Treated Electrodes. *J. Appl. Phys.* **2006**, *100*, 114517.

(17) Campbell, I. H.; Rubin, S.; Zawodzinski, T. A.; Kress, J. D.; Martin, R. L.; Smith, D. L.; Barashkov, N. N.; Ferraris, J. P. Controlling Schottky Energy Barriers in Organic Electronic Devices Using Self-Assembled Monolayers. *Phys. Rev. B* **1996**, *54*, R14321–R14324.

(18) Waske, P.; Wächter, T.; Terfort, A.; Zharnikov, M. Nitro-Substituted Aromatic Thiolate Self-Assembled Monolayers: Structural Properties and Electron Transfer upon Resonant Excitation of the Tail Group. *J. Phys. Chem. C* **2014**, *118*, 26049–26060.
(19) Xie, Y.; Cai, S.; Shi, Q.; Ouyang, S.; Lee, W.-Y.; Bao, Z.; Matthews, J. R.; Bellman, R. A.; He, M.; Fong, H. H. High Performance Organic Thin Film Transistors Using Chemically Modified Bottom Contacts and Dielectric Surfaces. *Org. Electron.* **2014**, *15*, 2073–2078.
(20) Fracasso, D.; Muglali, M. I.; Rohwerder, M.; Terfort, A.; Chiechi, R. C. Influence of an Atom in EGaIn/Ga2O3 Tunneling Junctions Comprising Self-Assembled Monolayers. *J. Phys. Chem. C* **2013**, *117*, 11367–11376.
(21) Kim, H.; Meihui, Z.; Battaglini, N.; Lang, P.; Horowitz, G. Large Enhancement of Hole Injection in Pentacene by Modification of Gold with Conjugated Self-Assembled Monolayers. *Org. Electron.* **2013**, *14*, 2108–2113.
(22) Hamadani, B. H.; Corley, D. A.; Ciszek, J. W.; Tour, J. M.; Natelson, D. Controlling Charge Injection in Organic Field-Effect Transistors Using Self-Assembled Monolayers. *Nano Lett.* **2006**, *6*, 1303–1306.
(23) Zhang, T.; Ma, Z.; Wang, L.; Xi, J.; Shuai, Z. Interface Electronic Structures of Reversible Double-Docking Self-Assembled Monolayers on an Au(111) Surface. *Philos. Trans. R. Soc. Lond. Math. Phys. Eng. Sci.* **2014**, *372*, 20130018.
(24) Benassi, E.; Corni, S. Work Function Changes of Azo-Derivatives Adsorbed on a Gold Surface. *J. Phys. Chem. C* **2014**, *118*, 26033–26040.
(25) Hofmann, O. T.; Egger, D. A.; Zojer, E. Work-Function Modification beyond Pinning: When Do Molecular Dipoles Count? *Nano Lett.* **2010**, *10*, 4369–4374.
(26) Egger, D. A.; Rissner, F.; Rangger, G. M.; Hofmann, O. T.; Wittwer, L.; Heimel, G.; Zojer, E. Self-Assembled Monolayers of Polar Molecules on Au(111) Surfaces: Distributing the Dipoles. *Phys. Chem. Chem. Phys.* **2010**, *12*, 4291.
(27) Rissner, F.; Rangger, G. M.; Hofmann, O. T.; Track, A. M.; Heimel, G.; Zojer, E. Understanding the Electronic Structure of Metal/SAM/Organic−Semiconductor Heterojunctions. *ACS Nano* **2009**, *3*, 3513–3520.
(28) Wang, L.; Rangger, G. M.; Romaner, L.; Heimel, G.; Bučko, T.; Ma, Z.; Li, Q.; Shuai, Z.; Zojer, E. Electronic Structure of Self-Assembled Monolayers on Au(111) Surfaces: The Impact of Backbone Polarizability. *Adv. Funct. Mater.* **2009**, *19*, 3766–3775.
(29) Sun, Q.; Selloni, A. Interface and Molecular Electronic Structure vs Tunneling Characteristics of CH3- and CF3-Terminated Thiol Monolayers on Au(111). *J. Phys. Chem. A* **2006**, *110*, 11396–11400, Erratum *J. Phys. Chem. A* **2007**, *111*, 10170.
(30) Anna M. Track, F. R. Simultaneously Understanding the Geometric and Electronic Structure of Anthraceneselenolate on Au(111): A Combined Theoretical and Experimental Study. *J. Phys. Chem. C* **2010**, *114*. Erratum *J. Phys. Chem. C* **2010**, *114*, 12838.
(31) Stammer, X.; Tonigold, K.; Bashir, A.; Käfer, D.; Shekhah, O.; Hülsbusch, C.; Kind, M.; Groß, A.; Wöll, C. A Highly Ordered, Aromatic Bidentate Self-Assembled Monolayer on Au(111): A Combined Experimental and Theoretical Study. *Phys. Chem. Chem. Phys.* **2010**, *12*, 6445.
(32) Otálvaro, D.; Veening, T.; Brocks, G. Self-Assembled Monolayer Induced Au(111) and Ag(111) Reconstructions: Work Functions and Interface Dipole Formation. *J. Phys. Chem. C* **2012**, *116*, 7826–7837.
(33) Cyganik, P.; Buck, M.; Wilton-Ely, J. D. E. T.; Wöll, C. Stress in Self-Assembled Monolayers: Ω-Biphenyl Alkane Thiols on Au(111). *J. Phys. Chem. B* **2005**, *109*, 10902–10908.

(34) Yuan, L.; Jiang, L.; Thompson, D.; Nijhuis, C. A. On the Remarkable Role of Surface Topography of the Bottom Electrodes in Blocking Leakage Currents in Molecular Diodes. *J. Am. Chem. Soc.* **2014**, *136*, 6554–6557.
(35) Berger, R.; Delamarche, E.; Lang, H. P.; Gerber, C.; Gimzewski, J. K.; Meyer, E.; Güntherodt, H.-J. Surface Stress in the Self-Assembly of Alkanethiols on Gold. *Science* **1997**, *276*, 2021–2024.
(36) Godin, M.; Williams, P. J.; Tabard-Cossa, V.; Laroche, O.; Beaulieu, L. Y.; Lennox, R. B.; Grütter, P. Surface Stress, Kinetics, and Structure of Alkanethiol Self-Assembled Monolayers. *Langmuir* **2004**, *20*, 7090–7096.
(37) Nouchi, R.; Shigeno, M.; Yamada, N.; Nishino, T.; Tanigaki, K.; Yamaguchi, M. Reversible Switching of Charge Injection Barriers at Metal/organic-Semiconductor Contacts Modified with Structurally Disordered Molecular Monolayers. *Appl. Phys. Lett.* **2014**, *104*, 013308.
(38) Lahann, J.; Mitragotri, S.; Tran, T.-N.; Kaido, H.; Sundaram, J.; Choi, I. S.; Hoffer, S.; Somorjai, G. A.; Langer, R. A Reversibly Switching Surface. *Science* **2003**, *299*, 371–374.
(39) Kuzumoto, Y.; Kitamura, M. Work Function of Gold Surfaces Modified Using Substituted Benzenethiols: Reaction Time Dependence and Thermal Stability. *Appl. Phys. Express* **2014**, *7*, 035701.
(40) Natan, A.; Kuritz, N.; Kronik, L. Polarizability, Susceptibility, and Dielectric Constant of Nanometer-Scale Molecular Films: A Microscopic View. *Adv. Funct. Mater.* **2010**, *20*, 2077–2084.
(41) Romaner, L.; Heimel, G.; Zojer, E. Electronic Structure of Thiol-Bonded Self-Assembled Monolayers: Impact of Coverage. *Phys. Rev. B* **2008**, *77*, 045113.
(42) Cornil, D.; Olivier, Y.; Geskin, V.; Cornil, J. Depolarization Effects in Self-Assembled Monolayers: A Quantum-Chemical Insight. *Adv. Funct. Mater.* **2007**, *17*, 1143–1148.
(43) Natan, A.; Zidon, Y.; Shapira, Y.; Kronik, L. Cooperative Effects and Dipole Formation at Semiconductor and Self-Assembled-Monolayer Interfaces. *Phys. Rev. B* **2006**, *73*, 193310.
(44) Hong, S.-Y.; Yeh, P.-C.; Dadap, J. I.; Osgood, R. M. Interfacial Dipole Formation and Surface-Electron Confinement in Low-Coverage Self-Assembled Thiol Layers: Thiophenol and P-Fluorothiophenol on Cu(111). *ACS Nano* **2012**, *6*, 10622–10631.
(45) Zhou, J.; Yang, Y. X.; Liu, P.; Camillone, N.; White, M. G. Electronic Structure of the Thiophene/Au(111) Interface Probed by Two-Photon Photoemission. *J. Phys. Chem. C* **2010**, *114*, 13670–13677.
(46) Di Castro, V.; Bussolotti, F.; Mariani, C. The Evolution of Benzenethiol Self-Assembled Monolayer on the Cu(1 0 0) Surface. *Surf. Sci.* **2005**, *598*, 218–225.
(47) Azzam, W.; Fuxen, C.; Birkner, A.; Rong, H.-T.; Buck, M.; Wöll, C. Coexistence of Different Structural Phases in Thioaromatic Monolayers on Au(111). *Langmuir* **2003**, *19*, 4958–4968.
(48) Leung, T. Y. B.; Schwartz, P.; Scoles, G.; Schreiber, F.; Ulman, A. Structure and Growth of 4-Methyl-4′-Mercaptobiphenyl Monolayers on Au(111): A Surface Diffraction Study. *Surf. Sci.* **2000**, *458*, 34–52.
(49) Liu, W.; Tkatchenko, A.; Scheffler, M. Modeling Adsorption and Reactions of Organic Molecules at Metal Surfaces. *Acc. Chem. Res.* **2014**, *47*, 3369–3377.
(50) Ramalho, J. P. P.; Gomes, J. R. B.; Illas, F. Accounting for van Der Waals Interactions between Adsorbates and Surfaces in Density Functional Theory Based Calculations: Selected Examples. *RSC Adv.* **2013**, *3*, 13085.
(51) Kresse, G.; Furthmüller, J. Efficient Iterative Schemes for Ab Initio Total-Energy Calculations Using a Plane-Wave Basis Set. *Phys. Rev. B* **1996**, *54*, 11169–11186.

(52) Perdew, J. P.; Burke, K.; Ernzerhof, M. Generalized Gradient Approximation Made Simple. *Phys. Rev. Lett.* **1996**, *77*, 3865–3868.
(53) Tkatchenko, A.; Scheffler, M. Accurate Molecular Van Der Waals Interactions from Ground-State Electron Density and Free-Atom Reference Data. *Phys. Rev. Lett.* **2009**, *102*, 073005.
(54) Ruiz, V. G.; Liu, W.; Zojer, E.; Scheffler, M.; Tkatchenko, A. Density-Functional Theory with Screened van Der Waals Interactions for the Modeling of Hybrid Inorganic-Organic Systems. *Phys. Rev. Lett.* **2012**, *108*, 146103.
(55) Al-Saidi, W. A.; Voora, V. K.; Jordan, K. D. An Assessment of the vdW-TS Method for Extended Systems. *J. Chem. Theory Comput.* **2012**, *8*, 1503–1513.
(56) Kresse, G.; Joubert, D. From Ultrasoft Pseudopotentials to the Projector Augmented-Wave Method. *Phys. Rev. B* **1999**, *59*, 1758–1775.
(57) Blöchl, P. Projector Augmented-Wave Method. *Phys. Rev. B* **1994**, *50*, 17953–17979.
(58) Monkhorst, H. J.; Pack, J. D. Special Points for Brillouin-Zone Integrations. *Phys. Rev. B* **1976**, *13*, 5188–5192.
(59) Neugebauer, J.; Scheffler, M. Adsorbate-Substrate and Adsorbate-Adsorbate Interactions of Na and K Adlayers on Al(111). *Phys. Rev. B* **1992**, *46*, 16067–16080.
(60) Bučko, T.; Hafner, J.; Ángyán, J. G. Geometry Optimization of Periodic Systems Using Internal Coordinates. *J. Chem. Phys.* **2005**, *122*, 124508.
(61) Rissner, F. Collective Effects in Self-Assembled Monolayers of Polar Organic Molecules. Doctoral Thesis, Graz University of Technology, 2012.
(62) Tao, Y.-T.; Wu, C.-C.; Eu, J.-Y.; Lin, W.-L.; Wu, K.-C.; Chen, C. Structure Evolution of Aromatic-Derivatized Thiol Monolayers on Evaporated Gold. *Langmuir* **1997**, *13*, 4018–4023.
(63) Bashir, A.; Käfer, D.; Müller, J.; Wöll, C.; Terfort, A.; Witte, G. Selenium as a Key Element for Highly Ordered Aromatic Self-Assembled Monolayers. *Angew. Chem. Int. Ed.* **2008**, *47*, 5250–5252.
(64) Käfer, D.; Witte, G.; Cyganik, P.; Terfort, A.; Wöll, C. A Comprehensive Study of Self-Assembled Monolayers of Anthracenethiol on Gold: Solvent Effects, Structure, and Stability. *J. Am. Chem. Soc.* **2006**, *128*, 1723–1732.
(65) Natan, A.; Kronik, L.; Haick, H.; Tung, R. T. Electrostatic Properties of Ideal and Non-Ideal Polar Organic Monolayers: Implications for Electronic Devices. *Adv. Mater.* **2007**, *19*, 4103–4117.
(66) Rusu, P. C.; Brocks, G. Work Functions of Self-Assembled Monolayers on Metal Surfaces by First-Principles Calculations. *Phys. Rev. B* **2006**, *74*, 073414.
(67) De Renzi, V.; Rousseau, R.; Marchetto, D.; Biagi, R.; Scandolo, S.; del Pennino, U. Metal Work-Function Changes Induced by Organic Adsorbates: A Combined Experimental and Theoretical Study. *Phys. Rev. Lett.* **2005**, *95*, 046804.
(68) Sushko, M. L.; Shluger, A. L. Intramolecular Dipole Coupling and Depolarization in Self-Assembled Monolayers. *Adv. Funct. Mater.* **2008**, *18*, 2228–2236.
(69) Deutsch, D.; Natan, A.; Shapira, Y.; Kronik, L. Electrostatic Properties of Adsorbed Polar Molecules: Opposite Behavior of a Single Molecule and a Molecular Monolayer. *J. Am. Chem. Soc.* **2007**, *129*, 2989–2997.
(70) Gershevitz, O.; Sukenik, C. N.; Ghabboun, J.; Cahen, D. Molecular Monolayer-Mediated Control over Semiconductor Surfaces: Evidence for Molecular Depolarization of Silane Monolayers on Si/SiOx. *J. Am. Chem. Soc.* **2003**, *125*, 4730–4731.
(71) Heimel, G.; Romaner, L.; Brédas, J.-L.; Zojer, E. Interface Energetics and Level Alignment at Covalent Metal-Molecule Junctions: Π-Conjugated Thiols on Gold. *Phys. Rev. Lett.* **2006**, *96*, 196806.

(72) Wang, L.; Rangger, G. M.; Ma, Z.; Li, Q.; Shuai, Z.; Zojer, E.; Heimel, G. Is There a Au–S Bond Dipole in Self-Assembled Monolayers on Gold? *Phys. Chem. Chem. Phys.* **2010**, *12*, 4287.
(73) Technically, this is achieved by calculating $\Delta\Phi$' for the combined metal/SAM system and $\Delta\Phi_{mol}$' for the (hypothetical) free standing monolayer. As $\Delta\Phi' = \Delta\Phi_{mol}' + \Delta\Phi_{BD}'$, $\Delta\Phi_{BD}'$ can then be obtained as the difference of the two quantities.
(74) Terentjevs, A.; Steele, M. P.; Blumenfeld, M. L.; Ilyas, N.; Kelly, L. L.; Fabiano, E.; Monti, O. L. A.; Della Sala, F. Interfacial Electronic Structure of the Dipolar Vanadyl Naphthalocyanine on Au(111): "Push-Back" vs Dipolar Effects. *J. Phys. Chem. C* **2011**, *115*, 21128–21138.
(75) Osikowicz, W.; Jong, M. P. de; Braun, S.; Tengstedt, C.; Fahlman, M.; Salaneck, W. R. Energetics at Au Top and Bottom Contacts on Conjugated Polymers. *Appl. Phys. Lett.* **2006**, *88*, 193504.
(76) Witte, G.; Lukas, S.; Bagus, P. S.; Wöll, C. Vacuum Level Alignment at Organic/metal Junctions: "Cushion" Effect and the Interface Dipole. *Appl. Phys. Lett.* **2005**, *87*, 263502.
(77) Bagus, P. S.; Staemmler, V.; Wöll, C. Exchangelike Effects for Closed-Shell Adsorbates: Interface Dipole and Work Function. *Phys. Rev. Lett.* **2002**, *89*, 096104.
(78) Hofmann, O. T.; Rangger, G. M.; Zojer, E. Reducing the Metal Work Function beyond Pauli Pushback: A Computational Investigation of Tetrathiafulvalene and Viologen on Coinage Metal Surfaces. *J. Phys. Chem. C* **2008**, *112*, 20357–20365.
(79) Note that due to the thiolate-Au bonds also charge-density fluctuations perpendicular to the substrate surface can be resolved, when plotting $\Delta\rho$ averaged over planes parallel to the substrate surface. These, however, can be viewed as a series of comparably moderate dipoles rather than a single. particularly large one [71].

TOC